Molecular Modeling Based Mutagenesis Defines Ligand Binding and Specificity Determining Regions of Fibroblast Growth Factor Receptors†

Tamara E. Gray,‡ Miriam Eisenstein,§ Tova Shimon,‡ David Givol,‡ and Avner Yayon*,‡

Departments of Chemical Immunology and Chemical Services, Weizmann Institute of Science, Rehovot 76100, Israel

Received May 3, 1995; Revised Manuscript Received June 14, 1995⊗

ABSTRACT: The fibroblast growth factor receptor 2 (FGFR2) and the keratinocyte growth factor receptor (KGFR) have different ligand binding specificities despite differing only in the second half of their immunoglobulin-like (Ig-like) domain III. Three-dimensional model structures were generated for domain III on the basis of variable (V) Ig domains. The region that differs between the two receptors is predicted to include two loops: one connects β-strands *F*−*G* and is analogous to the complementarity determining region 3 (CDR3) of immunoglobulins; the other connects β-strands *D*−*E*. These regions were targeted for mutagenesis. Single mutations in the *F*−*G* loop were found to only slightly alter ligand binding, whereas a double mutant, KGFR Y_{345}→S,Q_{348}→I, acquired significant affinity for bFGF. Notably, the affinity of this double mutant KGFR for KGF and aFGF was essentially unaltered. A mutant FGFR2, in which the *D*−*E* β-hairpin (T_{319}TDKEI) is replaced with the KGFR *D*−*E* β-hairpin (S_{319}SNA), has 9-fold reduced affinity for bFGF. These results demonstrate that the *F*−*G* or CDR3 analogous loop in FGFRs plays a key role in determining ligand binding and specificity. In addition, however, the protein loop connecting β-strands *D* and *E* may also be involved in ligand binding. Several point mutations in FGFR2, shown recently to give rise to multiple inherited skeletal defects, are localized according to our models to the *F*−*G* or *D*−*E* loops of domain III. Our results strongly suggest that these naturally occurring mutations specifically alter ligand binding by FGFR2.

Binding of fibroblast growth factors (FGFs)[1] to their cell surface receptors elicits a variety of responses that include cell proliferation, differentiation, wound repair, and angiogenesis (Folkman & Klagsburn, 1987; Goldfarb, 1990). Four FGFRs (Fantl et al., 1993) have been cloned which encode glycoproteins with two or three extracellular immunoglobulin-like (Ig-like) domains (Williams & Barclay, 1988), a single transmembrane domain, and a tyrosine kinase cytoplasmic domain (Yarden & Ullrich, 1988). There are numerous variants of these receptors that are produced by alternative splicing or alternative polyadenylation of their primary transcripts [for reviews, see Givol and Yayon (1992) and Jaye et al. (1992)]. Alternative splicing in the third Ig-like domain is responsible for the exclusive binding of bFGF and KGF to FGFR2 and KGFR, respectively. There is further complexity when one considers the ligands for the FGFRs. To date, nine different FGF ligands have been identified [for review, see Baird (1994)] which bind with overlapping specificities to their receptors. All FGFs bind heparin (Shing et al., 1984), as do their receptors (Kan et al., 1993; Pantoliano et al., 1994). Moreover, heparan sulphates are essential for the assembly of higher order macromolecular complexes of FGF with FGFRs and for biological activity (Rapraeger et al., 1991; Yayon et al., 1991). The FGF−FGFR system is intriguing, since highly homologous receptors not only bind common ligands, such as acidic FGF, but, in addition, exhibit high specificity with regard to the binding of other FGFs.

In order to understand the molecular basis for this specificity and in the absence of a three-dimensional structure of FGFR, we have exploited the fact that the extracellular portion of FGFR, responsible for ligand binding, is composed of Ig-like domains. Ig-like domains have been classified (Williams & Barclay, 1988) as belonging to variable (V) or constant (C) 1 and 2 sets, with one of the major differences between sets being the number of β-strands, either 9 or 7, respectively. The Ig-like extracellular domains of human FGFR1 have previously been modeled on the basis of both C and V domain structures (Pantoliano et al., 1994; Xu et al., 1992). We find that the third Ig-like domain in mouse FGFR2 and KGFR is most similar to an Ig V-type domain (i.e., nine β-strands arranged as a sandwich of two antiparallel β-sheets linked by a disulfide bond), and we generated structural models based on this framework (Chothia et al., 1988). More recently, the structural classification of the Ig fold has become more complex [for review, see Bork et al. (1994)] and includes the definition of an additional Ig structural set, the I-set. I-set structures are similar to V domain structures yet contain features found only in C

† This work was supported by the Israel Academy of Sciences and Humanities, Israel Cancer Research Fund, The Minerva Foundation, and the Kimmelman Center for Biomolecular Structure and Assembly. T.E.G. is the recipient of a Wellcome Fellowship. D.G. is incumbent of the Oscar H. and Anne Altshuler Chair of Immunochemistry. A.Y. is incumbent of the Alvin and Gertrude Levine Career Development Chair of Cancer Research.

* Correspondence should be addressed to this author (telephone, 972-8-342696; Fax, 972-8-344141).

‡ Department of Chemical Immunology.

§ Department of Chemical Services.

⊗ Abstract published in *Advance ACS Abstracts,* July 15, 1995.

[1] Abbreviations: FGF, fibroblast growth factor; FGFR, FGF receptor; Ig, immunoglobulin; aFGF, acidic FGF; bFGF, basic FGF; KGF, keratinocyte growth factor; KGFR, KGF receptor; SDS−PAGE, sodium dodecyl sulfate−polyacrylamide gel electrophoresis; Hepes, *N*-(2-hydroxyethyl)piperazine-*N*′-2-ethanesulfonic acid; HNTG, 20 mM Hepes, pH 7.5, 150 mM NaCl, 1% Triton X-100, and 10% glycerol; CDR, complementarity determining region; V-type, variable type; C-type, constant type. The one-letter amino acid code is used throughout.

0006-2960/95/0434-10325$09.00/0

domains (Harpaz & Chothia, 1994). Our model structures for domain III of FGFR2 and KGFR, like the extracellular domains of many other adhesion molecules and cell surface receptors, appear to belong to the recently defined I-set of Ig domain structures (Harpaz & Chothia, 1994). This domain was the focus of our study since it apparently possesses all the information to specify KGF or bFGF binding, in the context of domain II which is identical between FGFR2 and KGFR (Miki et al., 1992; Yayon et al., 1992). Specific mutations introduced into the predicted $D-E$ and $F-G$ loops suggest an important role for these loops in determining ligand binding and specificity of FGFR2 and KGFR.

EXPERIMENTAL PROCEDURES

Materials. Anti-alkaline phosphatase antibodies were from Zymed Laboratories Inc. (San Francisco, CA). Recombinant, bacterially expressed aFGF and bFGF were from Lederle (Pearl River, NY). KGF was from Pepro Tech Inc. (Rocky Hill, NJ). Geneticin was from Gibco/BRL (Gaithersberg, MD). Restriction and DNA modification enzymes were from New England Biolabs (Beverly, MA) or Boehringer (Mannheim, Germany). Heparin was from Hepar Industries (Franklin, OH). The mutagenesis kit was from Amersham International plc (Buckinghamshire, U.K.). Protein A−Sepharose was from Repligen (Cambridge, MA). Heparin−Sepharose was from Pharmacia (Uppsala, Sweden). Disuccinimidyl suberate was from Pierce Chemical Co. (Rockford, IL). All other chemicals were obtained from Sigma (St. Louis, MO).

Sequence Alignment. The number of residues between the conserved cysteines in the FGFR2 or KGFR third domain is greater than 60 (64 and 62, respectively), which is characteristic for a V-type Ig domain. In C-type domains the number of residues between the two cysteines is usually between 55 and 60 residues (Williams & Barclay, 1988). The alignment of KGFR (Figure 1B) with the Ig V domain was, therefore, based on the β-sheet framework structure of Ig V domain light chains (Chothia et al., 1988). The numbering of amino acids in the alignment (Figure 1B) is the same as that used for light chain Ig domains (Chothia et al., 1988) and is, therefore, not always consecutive, especially in the loop regions. The most conserved positions along the chain are the two cysteines in strands B and F and the tryptophan in strand C. These define well the B, C, and F strands and the $B-C$ loop, analogous to CDR1 in immunoglobulins. The alignment of β-strands A and A' and the loop between strands A' and B was obtained by following the sequence backward from position 19 (at the N terminus of β-strand B). The requirement for glycine at position 16 is satisfied whereas the requirement for glutamate or glutamine at position 6 was ignored as the structure of the N terminus of domain III is likely to be affected by the nearby connection to domain II. An acceptable alignment for position 35 (conserved tryptophan) onward was obtained only after shortening β-strand C' by one residue, resulting in a tyrosine at position 47 and a glycine at position 48. Alignment of the loop between β-strands C' and D (analogous to Ig CDR2) was based mainly on the requirement for a positively charged residue at position 61 near the end of the $C'-D$ loop, which forms a salt bridge with the conserved acidic residue at position 82. The structure defined by strands A, A', B, C, and C' is identical between FGFR2 and KGFR (Figure 1A). Strands D and E of FGFR2 and KGFR sequences fulfill most of the expected structural requirements as outlined by Chothia et al. (1988). The exception is at position 71 where there is a glutamate instead of a hydrophobic residue. The $D-E$ β-hairpin is longer by two residues in FGFR2 than in KGFR. The loop between strands E and F is dictated by the second cysteine. Positions 78 and 82 in this loop are aliphatic hydrophobic and acidic, respectively, as expected. Strand F includes the highly conserved cysteine and tyrosine residues at positions 86 and 88, respectively. The length of the loop between strands F and G (analogous to CDR3 in Ig) is difficult to determine in the absence of the expected highly conserved glycines at positions 99 and 101 in strand G. Nevertheless, the length of the $F-G$ loop is limited by the nearby C terminus of domain III. The seven identical residues between KGFR and FGFR2 from position 97 to position 104, including residues 102 and 104 which are highly conserved in the Ig family, are taken to form β-strand G. Position 106 is not conserved and may be affected by its proximity to the cell membrane.

Molecular Modeling. An initial model for KGFR was built according to the proposed alignment (Figure 1B), using the program ABMOD (M. Levitt). The program checks the sequence homology of fragments of the modeled structure (β-strands and loops) against corresponding fragments in several immunoglobulins of known structure. The model structure was built using the best matching fragments and was further refined by energy minimization with restraints on the backbone C_α positions using the program ENCAD (Levitt, 1983). The initial model for FGFR2 was based on the refined model for KGFR. The necessary replacements and deletions were performed using the program FRODO (Jones, 1978). Energy minimization was also performed on this model, restraining the C_α positions. Initially, all the loops were built in analogy to the immunoglobulins except the $F-G$ loop, which was made similar to the analogous loop in the C-terminal domain of the human growth hormone receptor (entry 3HHR in the protein data base; Abola et al., 1987). Further adjustments were made to the $B-C$ and $C'-D$ loops by applying dynamics to these regions alone (Figure 2).

Mutagenesis. Oligonucleotide-directed mutagenesis of FGFR2 and KGFR was performed using the Amersham kit on DNA encoding the extracellular portion of the receptor subcloned into M13mp8. The following oligonucleotides were used in the mutagenesis reactions (Figure 1A) (mismatches are underlined): 5′-GCGGGTAATGCTATCGGGATATC-3′ (FGFR2 $S_{347}\rightarrow$A), 5′-GGTCTCCAATTCTATAGGGCAGG-3′ (KGFR $Y_{345}\rightarrow$S), 5′-TTCTATAGGGATAGCCAACCAG-3′ (KGFR $Y_{345}\rightarrow$S,$Q_{348}\rightarrow$I), and 5′-CCGCCGGTGTTAACAGCTCGAATTGCAGAGGTTCTCTATATTC-3′ (FGFR2 T_{319}TDKEI→SSNA). The sequence of the mutants was confirmed using an ABI (Foster City, CA) automatic DNA sequencer.

Cell Transfection and Protein Expression. The extracellular portion of the mutated receptor was subcloned into the Aptag mammalian expression vector (Flanagan & Leder, 1990) to facilitate expression and secretion of the soluble receptor−alkaline phosphatase fusion protein. Transient expression of soluble receptors was achieved in COS 1 cells by electroporation with 10−20 μg of plasmid DNA using a Bio-Rad electroporator (250 V, 500 μF). Stable clones of NIH 3T3 and LE293 cells expressing soluble receptors were

generated by cotransfection with a neomycin resistance plasmid (Yayon et al., 1992) and selection in 800 μg/mL of geneticin. Conditioned medium from cells expressing the soluble receptors was heat inactivated at 65 °C and assayed for alkaline phosphatase activity as described previously (Flanagan & Leder, 1990).

Iodination of FGF Ligands and Chemical Cross-Linking. aFGF, bFGF, and KGF (2 μg) were iodinated by the chloramine T method (McConahey & Dixon, 1980) and purified on heparin−Sepharose. The specific activity was approximately 2×10^5 cpm/ng. Disuccinimidyl suberate (DSS) was used to cross-link 2 ng of ^{125}I-FGF to the soluble receptor immobilized with anti-alkaline phosphatase antibodies in the presence of 2 μg/mL heparin, essentially as described (Yayon et al., 1992). Cross-linked products were separated by SDS−PAGE on a 6% gel and visualized by autoradiography.

Receptor Binding to Heparin-Immobilized Ligand. FGF (100 ng) was incubated with a heparin−Sepharose slurry (30 μL) in phosphate-buffered saline (PBS, pH 7.4) (100 μL) at room temperature for 1 h. The FGF-bound heparin−Sepharose beads were washed three times with 20 mM Hepes, pH 7.5, 150 mM NaCl, 1% Triton X-100, and 10% glycerol (HNTG) before the addition of soluble receptor containing medium (200 μL). The initial receptor concentration was normalized for alkaline phosphatase activity. The beads were shaken at room temperature for 4 h and then washed three times with HNTG and once with 0.5 M NaCl before being assayed for alkaline phosphatase activity (Flanagan & Leder, 1990).

Direct Binding Assays. Soluble receptors normalized for alkaline phosphatase activity were immunoprecipitated from conditioned medium by incubation with anti-alkaline phophatase antibodies bound to protein A−Sepharose. The beads were then shaken at room temperature with various concentrations of ^{125}I-FGF in binding buffer containing 0.2% BSA, 25 mM HEPES, pH 7.4, 1% Tween-20, and 10 μg/mL heparin for at least 4 h. The beads were washed three times with HNTG and once with 0.5 M NaCl prior to being counted in a γ counter. Each assay was performed in duplicate.

Data Analysis. Apparent dissociation constants were determined by fitting the data directly using Kaleidagraph (version 2.1, Synergy Software PCS Inc.) to the equation

$$[RL] = \frac{[R_0][L]}{K_{app} + [L]} + c[L] \quad (1)$$

where $[R_0]$, $[L]$, and $[RL]$ represent the total receptor concentration, the free growth factor concentration, and the concentration of the growth factor−receptor complex, respectively. K_{app} is the apparent equilibrium dissociation constant, and c is the slope which reflects nonspecific binding. Equation 1 describes binding of ligand to a single site on a protein (Fersht, 1985) and includes a term to account for nonspecific binding. Dissociation constants determined from Scatchard analyses (not shown) were found to be in good agreement with those obtained from direct fitting to eq 1.

Competition Analysis. Displacement of ^{125}I-KGF (0.4 ng) from soluble receptor immobilized with anti-alkaline phosphatase antibodies was performed in a final volume of 100 μL of binding buffer containing 2 μg/mL heparin, with increasing concentrations of unlabeled ligand, with shaking at room temperature for 1 h. The beads were washed with HNTG and once with 0.5 M NaCl before being counted in a γ counter.

RESULTS

Sequence Alignment of KGFR and FGFR2 Membrane Proximal Domains with Immunoglobulin Variable Chains. The sequence alignment (Figure 1) was originally based on the framework structure outlined by Chothia et al. (1988) and is consistent with a more recently defined V-frame structural profile (Harpaz & Chothia, 1994). Alternative residues at 24 positions buried in the β-sheet and 6 residues in the turns of 7 immunoglobulin structures with known atomic coordinates were identified (Chothia et al., 1988). This enabled us to define "allowed" residues at these positions. Fifteen residues in both FGFR2 and KGFR were found corresponding to allowed buried β-sheet residues, and four out of six allowed turn residues were found in both receptors. These residues formed the basis of the alignment with the Ig variable domain (Figure 1B)

In a V-frame profile described more recently (Harpaz & Chothia, 1994) some 20 key framework residues are identified. These key residues have the same structural role in five Ig structures. Seventeen of the key residues are in β-strands and are mainly involved in the packing of the protein core; the remaining three key residues are in loop regions. Comparison of this new profile with both FGFR2 and KGFR third domains results in excellent matches with our alignments. The 3 conserved loop residues appear in domain III of both FGFR2 and KGFR and 14 of the conserved β-sheet residues also appear in both receptors. There are three discrepancies between the alignments shown (Figure 1B) and the V-frame profile described by Harpaz and Chothia (1994). A large hydrophobic residue with its side chain buried deep in the hydrophobic core is expected at position 48 (Figure 1B), whereas our alignment predicts a glycine residue. In the alignment presented here, however, the side chain of the neighboring tyrosine residue (position 47 in Figure 1B) is expected to be oriented into the hydrophobic core. The residue requirement at the position equivalent to 62 is satisfied in the case of FGFR2 with an alanine residue, whereas in KGFR there is a histidine (Figure 1B), which is a deviation from the most commonly found residues at this position (Harpaz & Chothia, 1994). At position 106 in the third domain of FGFR2 or KGFR (Figure 1B), there is a discrepancy with the V-frame profile (Harpaz & Chothia, 1994), but more importantly, position 104 in both FGFR2 and KGFR does fulfill the expected requirements and is predicted to penetrate deep into the hydrophobic core.

The primary sequences of KGFR and FGFR2 are identical except for the amino acid sequence of the membrane proximal domain III which includes a region with great variability. Inspection of the sequence comparison of this domain from KGFR and FGFR2 (Figure 1A) and the sequence alignment with the Ig V-domain framework structure (Figure 1B) reveals that the regions of least homology form the *F*−*G* loop (or CDR3 analogue) and the *D*−*E* β-hairpin. Regarding the latter, the β-hairpin is two amino acids shorter in KGFR than in FGFR2. Interestingly, there is one potential glycosylation site unique to the *F*−*G* loop of KGFR. The regions analogous to CDR1 (*B*−*C* loop) and CDR2 (*C*′−*D* loop) of Ig are completely conserved

A

```
FGFR2/      -A-   --A'-    ---B---        ---C----/---C'---
KGFR  (259) QAGLPANASTVVGGDVEFVCKVYSDAQPHIQWIKHVEKNGSKYGPDGLPYLKVLK (313)
                ---D---/---E---        ---F---        ----G----
FGFR2 (314) AAGVNTTDKEIEVLYIRNVTFEDAGEYTCLAGNSIGISFHSAWLTVLP...A (362)
                | |      |||   |||  |||||  |   | ||    ||||||||   |
KGFR  (314) HSGINSS..NAEVLALFNVTEMDAGEYICKVSNYIGQANQSAWLTVLPKQQA (363)
                ••••••                      *  *
```

B

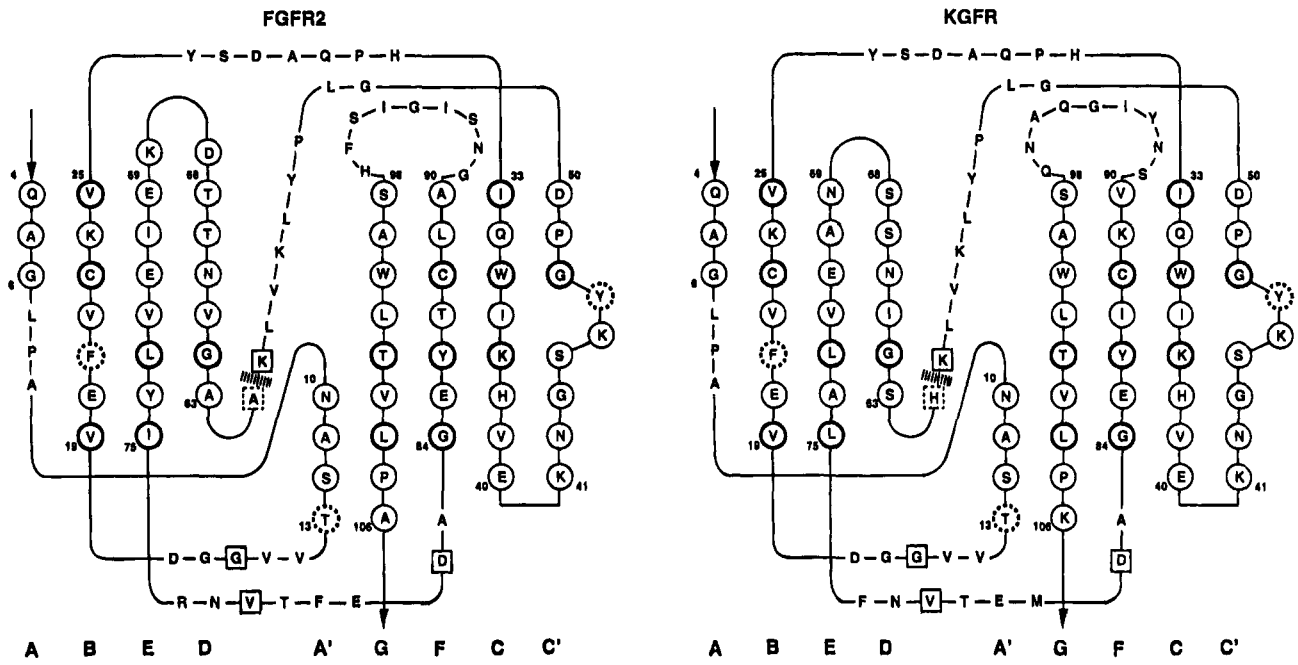

FIGURE 1: Amino acid sequence homology between the third extracellular domain of mouse KGFR and FGFR2 and alignment with the Ig V-domain framework structure. (A) Amino acid sequence of the third membrane proximal domain of KGFR and FGFR2. The sequence corresponding to the second half of the domain from both receptors is compared (exon IIIb/KGFR and exon IIIc/FGFR2), identical residues are connected by a vertical line, and the conserved cysteine residues are underlined. Regions predicted to form β-strands are indicated by a horizontal line above the sequence, and regions chosen for mutation in the *D*−*E* β-hairpin or the *F*−*G* loop are marked below the sequence (• or *, respectively). (B) Alignment of FGFR2 and KGFR third membrane proximal domains with the Ig light chain V-frame structure outlined by Chothia et al. (1988). Residues in circles represent framework structure residues, and those enclosed in heavy circles are "allowed" residues that are buried within the domain and have their side chains orientated into the β-sheet. The boxed amino acids represent residues that are highly conserved in variable Ig domain loops and also in the receptors. Residues with a broken circle or square represent acceptable conservative changes to "allowed" residues. Residues that do not correspond to framework structure residues and form connecting loops are depicted by letters with no surround. The hatched line represents the boundary corresponding to the alternatively spliced exon. Numbering is according to the variable Ig domain light chain sequence as described by Chothia et al. (1988) and is not necessarily consecutive. The individual β-strands are denoted by the letters in bold type at the bottom of the figure.

between the two receptors. Another feature of the alignment (Figure 1B) is that the two subdomains encoded by the alternatively spliced exons (Miki et al., 1992; Yayon et al., 1992) contain the following structural motifs: two-strand β-sheet−intervening loop−two-strand β-sheet. The two subdomains are structurally identical to the earliest "folding unit" proposed by McLachlan (1980). There is no suggestion from our alignment that domain III is involved in a quaternary structure similar to that found in antibodies since conserved residues (at positions 36, 38, 44, 46, 87, 89, and 98) involved in interdomain interactions in immunoglobulins (Chothia et al., 1988) are not found in domain III of either KGFR or FGFR2.

Three-Dimensional Models for FGFR2 and KGFR Third Extracellular Domains and Design of Mutations. A ribbon diagram depicting the three-dimensional model for KGFR is shown, and regions chosen for mutation are indicated (Figure 2A; see also Figure 1A). It may be seen that the loop connecting β-strands *D* and *E* (not analogous to a CDR of Ig) differs in both size and primary structure between KGFR and FGFR2 and faces in the same upward direction as the CDR analogues (Figure 2). On the basis of the three-dimensional models and sequence comparison between KGFR and FGFR2, we constructed the following four soluble receptors mutated in either the *F*−*G* loop or the *D*−*E* β-hairpin: FGFR2 S_{347}→A; KGFR Y_{345}→S; KGFR Y_{345}→S,Q_{348}→I; FGFR2 T_{319}TDKEI→SSNA.

Analysis of Binding of FGF Ligands to Soluble Receptors Mutated in the F−*G Loop.* ^{125}I-FGFs were cross-linked to the receptor mutants FGFR2 S_{347}→A, KGFR Y_{345}→S, and KGFR Y_{345}→S,Q_{348}→I in the presence or absence of excess unlabeled ligands. Cross-linking products corresponding to the soluble KGFR Y_{345}→S,Q_{348}→I mutant receptor bound to ^{125}I-KGF can be seen in Figure 3A. The higher mobility band corresponds to receptor monomer cross-linked to ^{125}I-KGF; the lower mobility band is ^{125}I-KGF cross-linked to receptor dimers. The cross-linking of ^{125}I-aFGF to the single mutant receptors in the presence or absence of an excess of various unlabeled ligands is not shown but was found to be the same as for the parental receptors (Yayon et al., 1992). In the case of the double mutant KGFR Y_{345}→S,Q_{348}→I, however, bFGF is much more effective at displacing ^{125}I-

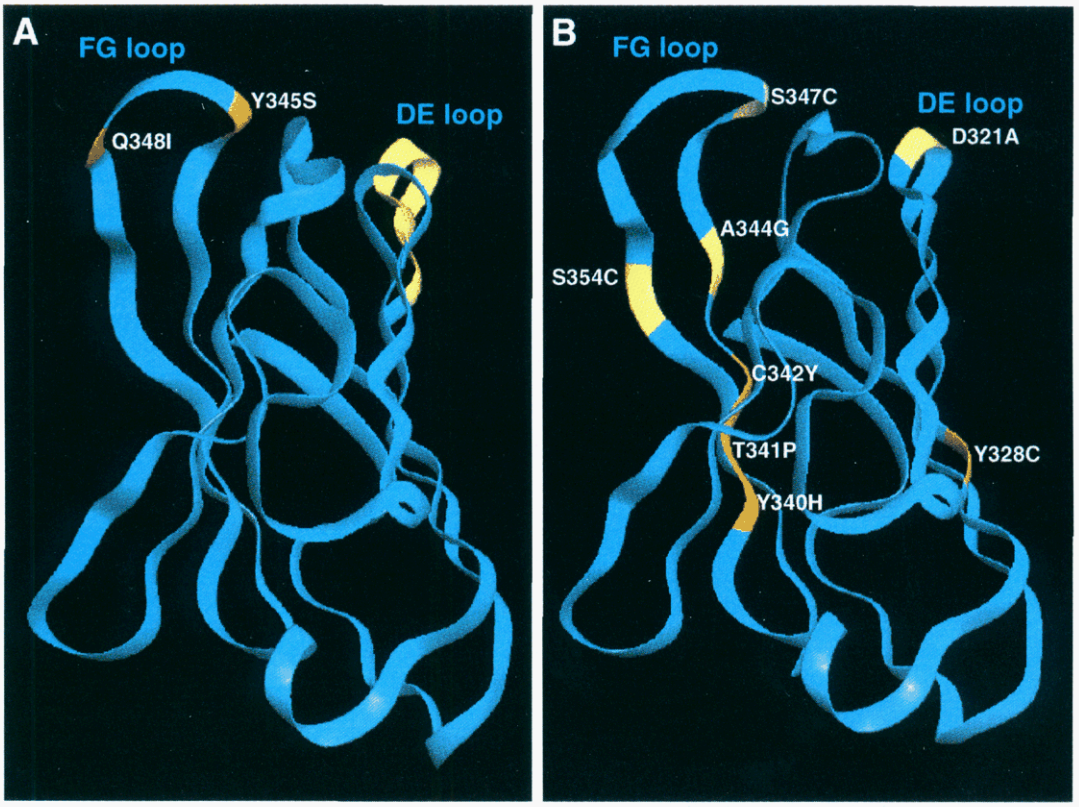

FIGURE 2: Ribbon diagrams depicting the C_α backbone of the model structures for domain III of KGFR and FGFR2. (A) KGFR domain III. Regions mutated in the *F*−*G* loop are shown in orange, and the longer *D*−*E* loop found in FGFR2 is superimposed on the shorter KGFR *D*−*E* loop, shown in yellow. (B) FGFR2 domain III. The positions of naturally occurring mutations responsible for various inherited skeletal abnormalities (Mulvihill, 1995) are colored. Mutations in the *F*−*G* and *D*−*E* loop regions are shown in yellow, and those occurring in the β-sheet framework structure are shown in orange.

KGF (Figure 3A) than was found for the parental KGFR. Strikingly, this double mutant can still specifically bind aFGF and KGF like the parental KGFR (Figure 3A). Binding of these *F*−*G* loop mutant receptors to FGF ligands immobilized on heparin−Sepharose followed by alkaline phosphatase assays (Figure 3B) indicates that both the single mutants FGFR2 S_{347}→A and KGFR Y_{345}→S specifically bind aFGF and either bFGF or KGF, respectively. The ability of the KGFR Y_{345}→S,Q_{348}→I double mutant to bind bFGF as well as aFGF and KGF is also reflected in this assay (Figure 3B), confirming the cross-linking results (Figure 3A).

In order to evaluate quantitatively the changes in affinity resulting from mutations introduced into the CDR3 analogues of KGFR and FGFR2, direct binding experiments were performed (Figure 4). The apparent binding constants obtained after analyzing the data, as described in Experimental Procedures, are summarized in Table 1. The binding affinity of the FGFR2 S_{347}→A mutant for aFGF is slightly reduced relative to that displayed by the wild-type receptor, whereas no change in affinity for aFGF is detectable for the KGFR Y_{345}→S mutant compared with KGFR. In these direct binding assays KGFR displays an approximately 5-fold higher affinity for aFGF than FGFR2. The binding affinity of the FGFR2 S_{347}→A mutant for bFGF is slightly increased (Table 1), whereas binding of KGF, as found for the wild-type receptor, is too weak to measure. The KGFR Y_{345}→S mutant is unaltered in its high affinity for KGF. These results indicate that the tyrosine and serine residues mutated in the *F*−*G* loops of KGFR and FGFR2, respectively, do not significantly affect ligand binding by either receptor. The modest effects seen for the FGFR2 S_{347}→A mutant may, however, reflect the conservative nature of the substitution but in addition suggest that this position may be involved in the binding of both aFGF and bFGF. The apparent binding constants obtained for the double mutant KGFR Y_{345}→S,Q_{348}→I show that this receptor has acquired affinity for bFGF, without markedly losing affinity for KGF and aFGF (Figure 4 and Table 1). Analysis of displacement curves (Figure 4D) confirms that the double mutant KGFR Y_{345}→S,Q_{348}→I and KGFR have similar affinity for KGF, but the double mutant has enhanced affinity for bFGF. The *F*−*G* loop may, therefore, play an important role in determining FGFR specificity.

Analysis of the Ligand Binding Characteristics of a Soluble Receptor Mutated in the Short D−*E Connecting Loop.* The *D*−*E* β-hairpin in domain III varies in both length and charge between FGFR2 and KGFR (Figures 1 and 2). The TTDKEI motif in the *D*−*E* β-hairpin of FGFR2 (residues 319−324) was replaced with the SSNA motif found at the equivalent position in KGFR (see Figure 1A). FGFR2 T_{319}-TDKEI→SSNA cross-linked to ^{125}I-aFGF in the presence or absence of excess cold ligand is shown (Figure 5A). Receptor monomers and dimers cross-linked to FGF correspond to higher and lower mobility bands, respectively. The relative amount of receptor dimers observed with ^{125}I-bFGF cross-linked to receptors (Figure 5A) is somewhat larger than observed for other ligands. This difference probably reflects small differences in cross-linking conditions between experiments. There is complete displacement of ^{125}I-aFGF with unlabeled aFGF and little or no displacement of ^{125}I-aFGF by unlabeled KGF. This is exactly as found previously for the wild-type receptor FGFR2 (Yayon et al.,

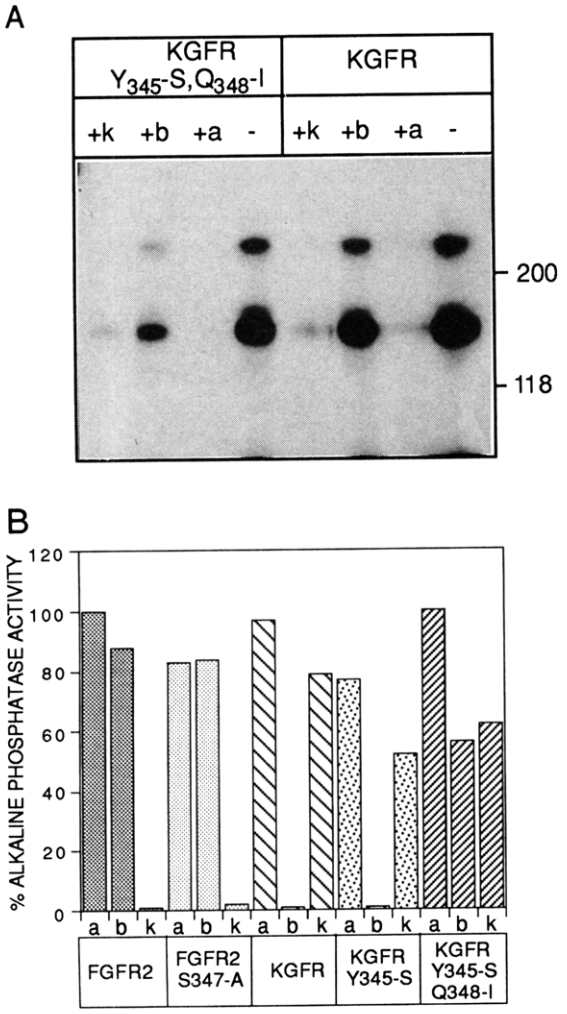

FIGURE 3: Autoradiograph of ^{125}I-KGF cross-linked to KGFR and the mutant receptor KGFR $Y_{345}\rightarrow S,Q_{348}\rightarrow I$. (A) ^{125}I-KGF cross-linked to KGFR $Y_{345}\rightarrow S,Q_{348}\rightarrow I$ and KGFR are shown on the left- and right-hand sides of the figure, respectively. The experiment was performed in the presence (+) or absence (−) of a 100-fold excess of unlabeled ligands: aFGF (a), bFGF (b), and KGF (k). (B) Ligand binding profile for FGFR2, KGFR, and three $F-G$ loop mutant receptors. Ligand binding is reflected by the relative amount of alkaline phosphatase activity associated with aFGF (a), bFGF (b), and KGF (k) immobilized on heparin−Sepharose beads.

1992). Notably, however, there is very little displacement of ^{125}I-aFGF by unlabeled bFGF. This is in contrast to the complete displacement of aFGF by bFGF observed for wild-type FGFR2 under the same conditions (Yayon et al., 1992), indicating that the $D-E$ loop in FGFR2 may significantly contribute to the binding of bFGF. The amount of receptor that may be cross-linked to ^{125}I-bFGF is also clearly less for the FGFR2 T_{319}TDKEI→SSNA mutant receptor compared to the wild type, confirming the reduced affinity for bFGF by this receptor mutant (Figure 5A).

Binding of the FGFR2 T_{319}TDKEI→SSNA mutant to FGF ligands immobilized on heparin−Sepharose beads followed by alkaline phosphatase assays (Figure 5B) confirms the cross-linking results. There is reduced bFGF binding and no evidence to suggest acquisition of KGF binding by the FGFR2 T_{319}TDKEI→SSNA mutant. The FGFR2 T_{319}-TDKEI→SSNA mutant binds to immobilized aFGF (Figure 5B), although with somewhat lower affinity than FGFR2. The affinity of this receptor for bFGF as determined from direct binding experiments is reduced 9-fold relative to the wild-type receptor (Table 1), indicating that in FGFR2 the TTDKEI sequence forming the $D-E$ loop probably participates in bFGF binding. The presence of the KGFR sequence SSNA in this $D-E$ loop is, however, clearly not sufficient to confer KGF binding onto FGFR2.

DISCUSSION

The overall protein fold of domain III in FGFR2 and KGFR is predicted from our sequence alignment to be similar to that of an Ig V-type domain (Chothia et al., 1988). The loop sequences analogous to CDRs, however, show no obvious similarity to the canonical sequences described for the hypervariable regions in immunoglobulins (Chothia et al., 1989). It nevertheless seemed likely, given the sequence diversity in this region and its apparent exposure to solvent (Figure 1B and 2), that FGF binding by these receptors might involve the $F-G$ loop, in analogy to the crucial role of CDR3 in antigen binding by immunoglobulins and to the human growth hormone receptor C-terminal domain (De Vos et al., 1992). We chose first to mutate residue 347 in the $F-G$ loop of FGFR2 and the corresponding residue (345) in KGFR (Figure 1A). A serine is found at this site in many FGFRs from different species, but uniquely, in KGFRs there is a tyrosine (see Figure 1). Tyrosine is commonly found in Ig CDRs [see, for example, Amit et al. (1986)] as well as in other specific protein−protein complexes, so we reasoned that serine or tyrosine at this position might contribute to the different ligand binding specificities of FGFR2 and KGFR. In FGFR2, changing serine at position 347 to an alanine residue resulted in reduced affinity for aFGF (3-fold) and a slight increase in affinity for bFGF. This could reflect the fact that this position participates in the binding of both ligands, and the serine residue in FGFR2 represents the best compromise for high-affinity binding of both aFGF and bFGF. There was, on the other hand, no detectable effect on the affinity of KGFR for either aFGF or KGF when the tyrosine residue at the equivalent position in the $F-G$ loop of KGFR was mutated to serine.

Glutamine at position 348 in KGFR is unique to KGF binding receptors, with the equivalent position in all other FGFRs being occupied by a hydrophobic residue. A double mutant, KGFR $Y_{345}\rightarrow S,Q_{348}\rightarrow I$, where this glutamine, in addition to the tyrosine residue mentioned above, is replaced with isoleucine, exhibits a strikingly different ligand binding specificity. This mutant acquired the capacity to bind bFGF, albeit with somewhat lower affinity than is found for KGF or aFGF, but it is at least 10-fold higher than that found for the parental receptor (Table 1). The $F-G$ loop in the third Ig-like domain of KGFR, therefore, plays an important functional role in ligand binding, as does the analogous loop (CDR3) in antibodies. Our results are consistent with the molecular model put forward recently for bFGF binding to FGFR1 (Pantoliano et al., 1994), where the bFGF binding site is proposed to mimic the protein A binding site of Fc and includes the $F-G$ loop from domain III as well as two other loop regions from domain II. It is not clear, at this stage, whether the acquired affinity of the mutant receptor for bFGF is solely via a direct interaction with the growth factor or whether some of the effect is indirect due to a change in receptor affinity for heparin. Previous studies suggest that FGFRs bind directly to heparin mainly by a region in domain II of FGFR2 (Kan et al., 1993; Pantoliano et al., 1994). We find that the double mutant KGFR

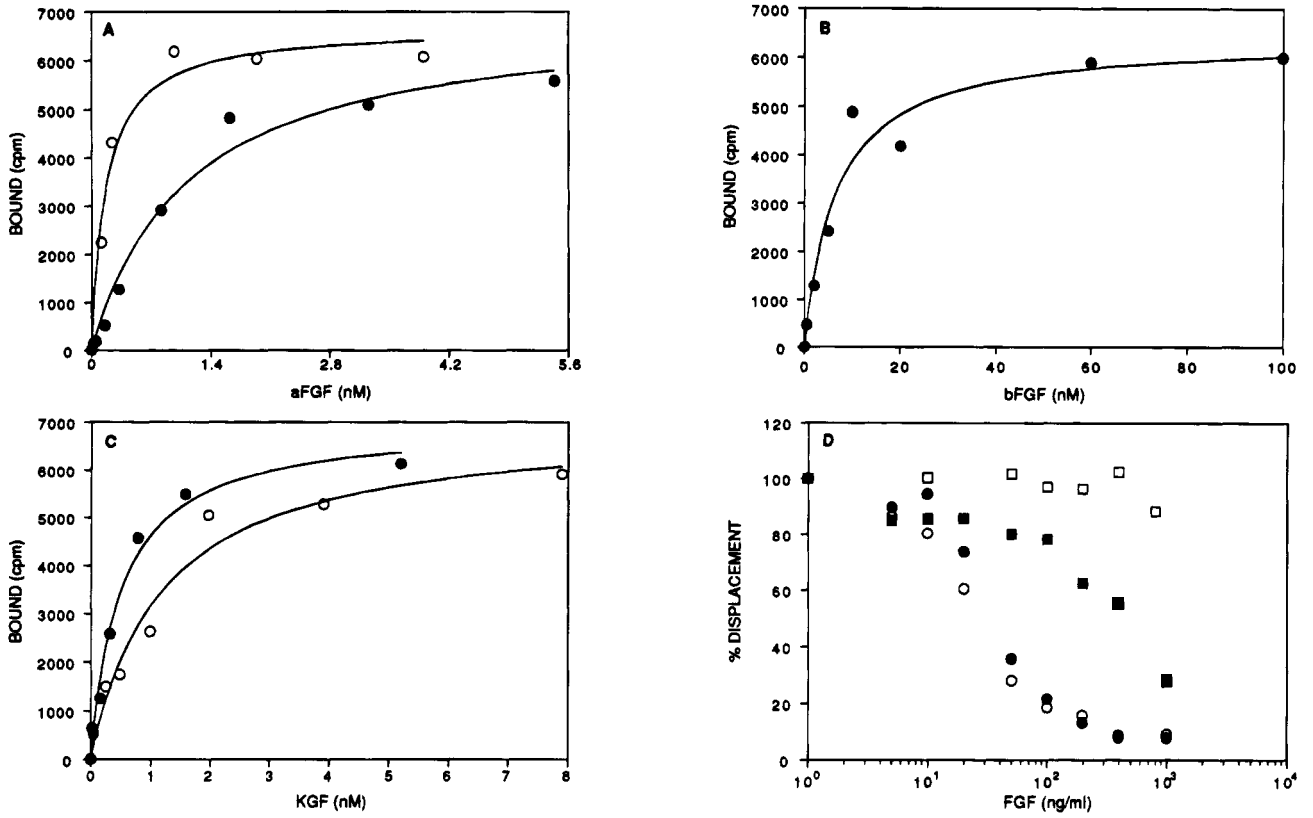

FIGURE 4: Direct binding of ^{125}I-FGFs to KGFR and the $F-G$ loop double mutant $Y_{345}\rightarrow S,Q_{348}\rightarrow I$ and displacement analyses. (A–C) Direct binding curves obtained for aFGF, bFGF, and KGF binding to KGFR $Y_{345}\rightarrow S,Q_{348}\rightarrow I$ (closed circles) and wild-type KGFR (open circles). The solid lines represent the best fit of the data to eq 1 after subtraction of the linear component due to nonspecific binding. For clarity, the data have been normalized such that the free receptor concentration (determined from the fit) is the same in each case. (D) ^{125}I-KGF displacement by unlabeled KGF (circles) or bFGF (squares) from KGFR (open symbols) or from mutant KGFR $Y_{345}\rightarrow S,Q_{348}\rightarrow I$ (closed symbols).

Table 1: Apparent Dissociation Constants (nM) Determined for Binding of ^{125}I-FGF Ligands to Soluble FGF Receptors[a]

FGF ligand	FGFR2	FGFR2 $S_{347}\rightarrow A$	KGFR	KGFR $Y_{345}\rightarrow S$	KGFR $Y_{345}\rightarrow S,Q_{348}\rightarrow I$	FGFR2 T_{319}TDKEI→SSNA
aFGF	2.5 ± 0.5	8.1 ± 1.5	0.5 ± 0.1	0.3 ± 0.1	1.1 ± 0.2	7.1 ± 0.6
bFGF	1.7 ± 0.1	1.2 ± 0.2	>50	nd	6.5 ± 1.8	16.1 ± 4.1
KGF	nd	nd	1.1 ± 0.5	1.2 ± 0.3	0.5 ± 0.1	nd

[a] Apparent binding constants were determined from direct binding measurements. The errors are determined by the fitting program. Affinity too low to measure is denoted as not determined (nd).

$Y_{345}\rightarrow S,Q_{348}\rightarrow I$ has a higher affinity for heparin than KGFR but the heparin dependence of KGF and bFGF binding to this mutant receptor (data not shown) mirrors that found for binding of these ligands to KGFR and FGFR2, respectively.

The other region of significant sequence diversity between FGFR2 and KGFR is in the loop connecting β-strands D and E, which does not correspond to a CDR in antibodies. Not only is the β-hairpin in KGFR shorter by two residues but it also lacks the charged lysine, aspartate, and glutamate residues present in the $D-E$ β-hairpin of FGFR2. We find that substitution of the four residues found in the KGFR $D-E$ β-hairpin for the six residues in the FGFR2 $D-E$ β-hairpin substantially reduces the affinity of FGFR2 for bFGF, with a lesser effect on aFGF binding. This result implies that the $D-E$ loop region of FGFR2 may contribute to bFGF binding by FGFR2. The reduced affinity of the mutant FGFR2 T_{319}TDKEI→SSNA for aFGF, a more promiscuous ligand than bFGF, suggests that it may also bind to this region. Previously, we showed that a chimeric receptor of FGFR2 containing residues 314–338 from KGFR in place of residues 314–340 in FGFR2 retains significant aFGF binding capacity but loses detectable affinity for bFGF (Yayon et al., 1995). The mutant FGFR2 T_{319}TDKEI→SSNA, therefore, displays ligand binding properties intermediate between those of the chimeric receptor and wild-type FGFR2 (Table 1). The binding site for bFGF in FGFR2 may map at least partially between residues 314 and 340 with a substantial portion of the binding energy attributable to the six-residue sequence TTDKEI (319–324) which forms the $D-E$ β-hairpin in FGFR2.

A peptide corresponding to amino acids 313–337 from KGFR (Figure 1A) was found to compete with KGFR for binding to KGF (Bottaro et al., 1993) although with >1000-fold reduced affinity. Consequently, this region was suggested to be involved in forming the KGFR ligand binding site. Interestingly, neither the FGFR2 T_{319}TDKEI→SSNA mutant nor the chimeric receptor (Yayon et al., 1995) acquired the capacity to bind KGF. These results suggest that other residues outside the sequence encompassed by residues 313–337 of KGFR may be required for KGF binding. Alternatively, there may be distinct negative determinants present in the mutant and chimeric receptors that restrict receptor–ligand interaction, as has been suggested for other receptor–ligand pairs (Moyle et al., 1994).

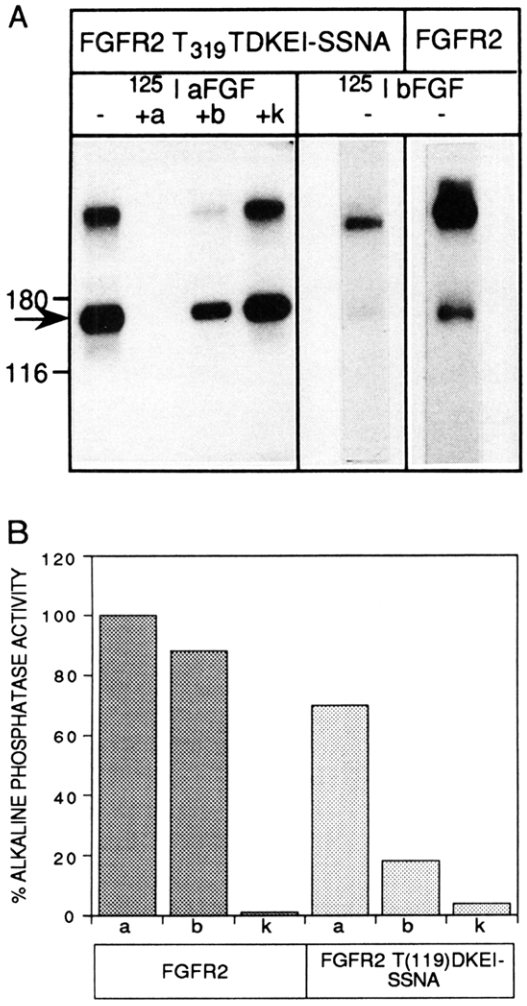

FIGURE 5: Binding analysis of the $D-E$ loop mutant receptor. (A) Autoradiograph of ^{125}I-FGFs cross-linked to FGFR2 and the mutant FGFR2 T_{319}TDKEI→SSNA. On the left-hand side ^{125}I-aFGF is cross-linked to the mutant receptor FGFR2 T_{319}TDKEI→SSNA in the absence (−) or presence (+) of excess unlabeled aFGF (a), bFGF (b), and KGF (k). On the right-hand side, the same concentration of ^{125}I-bFGF (2 ng) is cross-linked to FGFR2 and to the mutant receptor FGFR2 T_{319}TDKEI→SSNA. The arrow indicates receptor monomer cross-linked to FGF. (B) Ligand binding profile for FGFR2 and FGFR2 T_{319}TDKEI→SSNA. Ligand binding is reflected by the relative amount of alkaline phosphatase activity associated with aFGF (a), bFGF (b), and KGF (k) immobilized on heparin−Sepharose beads.

Previously, on the basis of binding experiments with chimeric FGFRs (Yayon et al., 1995), we suggested that regions in domain III predicted to contain the $D-E$ and $F-G$ β-strands in their respective connecting loops may interact with each other, either directly or indirectly *via* ligand. The findings reported here are consistent with this suggestion, since both $D-E$ and $F-G$ loops are implicated in the binding of bFGF. According to our model the loops analogous to CDRs 1 and 2 in immunoglobulins are completely conserved in the third domains of both FGFR2 and KGFR. Some of the binding energy involved in high-affinity ligand binding by KGFR and FGFR2 may arise from interactions of ligand with such regions that are conserved between the receptors. It has also been suggested that the second Ig-like domain participates in ligand binding by FGFRs (Pantoliano et al., 1994; Zimmer et al., 1993). Indeed, it has been reported that domain II provides the major high-affinity binding site for aFGF (Cheon et al., 1994). Here, we find that mutations in domain III affect aFGF binding, despite the presence of an unaltered second domain. It seems, therefore, that aFGF binding probably involves interactions with both domains II and III.

Recently, several dominantly inherited human skeletal disorders have been correlated with specific mutations in FGFRs (Erlebacher et al., 1995). The positions of these naturally occurring mutations in our model structure of FGFR2 domain III are shown in Figure 2B. Interestingly, the majority of the reported mutations in FGFR2 are localized to the F β-strand (Mulvihill, 1995). Of these, in at least 16 reported cases, the mutations map to the $F-G$ loop in domain III of FGFR2. In one other case the mutation is in the $D-E$ loop (Mulvihill, 1995). Moreover, the two cases reported for Pfeiffer and Crouzon's syndrome contain a $D-E$ loop mutation (D_{321}→A) and an $F-G$ loop mutation (S_{347}→C), respectively (Mulvihill, 1995): the same positions in FGFR2 have been mutated in this study (although to a different residue). Our findings, therefore, suggest that FGFR ligand binding sites are specifically altered in patients with these inherited skeletal displasias.

Molecular modeling combined with site-directed mutagenesis has allowed us to test whether recognition of FGF ligands may be considered analogous to antibody−antigen recognition. We present evidence suggesting that the $F-G$ loop in FGFR contains residues important in determining the specificity of ligand binding and its role does appear similar to that of the CDR3 in antibodies and the $F-G$ loop in the human growth hormone receptor C-terminal domain. In addition, however, the $D-E$ β-hairpin, apparently not important in antibody−antigen interactions, is also important for FGF binding. We, therefore, suggest that FGFR2, in common with some other cell surface receptors such as the human growth hormone receptor (Bork et al., 1994; De Vos et al., 1992), may use the immunoglobulin framework structure as a scaffold with which to bind ligands in a unique manner. More structural information, analysis of more mutants, and ultimately a three-dimensional structure of a heparin−FGF−FGFR complex should lead to a clearer understanding of the principles governing growth factor recognition by FGFRs.

ACKNOWLEDGMENT

We thank Michael Levitt for his advice and for the computer programs, Andrew Seddon for providing aFGF and bFGF, and Clive Dickson for the gift of COS 1 cells.

REFERENCES

Abola, E., Bernstein, F. C., Bryant, S. H., Koetzle, T. F., & Weng, J. (1987) in *Protein Data Bank in Crystallographic Data based-Information Content, Software Systems, Scientific Applications* (Allen, F. H., Bergerhoff, G., & Sievers, R., Eds.) pp 107−132, Data Commission of the International Union of Crystallography, Bonn/Cambridge/Chester.

Amit, A. G., Mariuzza, R. A., Phillips, S. E. V., & Poljak, R. J. (1986) *Science 233*, 747−753.

Baird, A. (1994) *Curr. Opin. Neurobiol. 4*, 78−76.

Bork, P., Holm, L., & Sander, C. (1994) *J. Mol. Biol. 242*, 309−320.

Bottaro, D. P., Fortney, E., Rubin, J. S., & Aaronson, S. A. (1993) *J. Biol. Chem. 268*, 9180−9193.

Cheon, H.-G., LaRochelle, W. J., Bottaro, D. P., Burgess, W. H., & Aaronson, S. A. (1994) *Proc. Natl. Acad. Sci. U.S.A. 91*, 989−993.

Chothia, C., Boswell, D. R., & Lesk, A. M. (1988) *EMBO J. 7*, 3745−3755.

Chothia, C., Lesk, A. M., Tramontano, A., Levitt, M., Smith-Gill, S. J., Air, G., Sheriff, S., Padlan, E. A., Davies, D., Tulip, W. R., Colman, P. M., Spinelli, S., Alzari, P. M., & Poljak, R. J. (1989) *Nature 342*, 877−883.

De Vos, A. M., Ultsch, M., & Kossiakoff, A. A. (1992) *Science 255*, 306−312.

Erlebacher, A., Filvaroff, E. H., Gitelman, S. E., & Derynck, R. (1995) *Cell 80*, 371−378.

Fantl, W. J., Johnson, D. E., & Williams, L. T. (1993) *Annu. Rev. Biochem. 62*, 453−481.

Fersht, A. R. (1985) *Enzyme Structure and Mechanism*, pp 190−191, W. H. Freeman and Co., New York.

Flanagan, J. G., & Leder, P. (1990) *Cell 63*, 185−194.

Folkman, J., & Klagsburn, M. (1987) *Science 235*, 442−447.

Givol, D., & Yayon, A. (1992) *FASEB J. 6*, 3362−3369.

Harpaz, Y., & Chothia, C. (1994) *J. Mol. Biol. 238*, 528−539.

Jaye, M., Schlessinger, J., & Dionne, C. A. (1992) *Biochim. Biophys. Acta 1135*, 185−199.

Jones, T. A. (1978) *J. Appl. Crystallogr. 11*, 268−272.

Kan, M., Wang, F., Xu, J., Crabb, J. W., Hou, J., & McKeehan, W. L. (1993) *Science 259*, 1918−1921.

Levitt, M. (1983) *J. Mol. Biol. 168*, 595−620.

McConahey, P. J., & Dixon, F. J. (1980) *Methods Enzymol. 70*, 210−213.

McLachlan, A. (1980) *Protides of the Biological Fluids* (Peters, H., Ed.) pp 29−32, Pergamon Press, New York.

Miki, T., Bottaro, D. P., Fleming, T. P., Smith, C. L., Burgess, W. H., Chan, A. M., & Aaronson, S. A. (1992) *Proc. Natl. Acad. Sci. U.S.A. 89*, 246−250.

Moyle, W. R., Campbell, R. K., Myers, R. V., Bernard, M. P., Han, Y., & Wang, X. (1994) *Nature 368*, 251−255.

Mulvihill, J. J. (1995) *Nature Genet. 9*, 101−103.

Pantoliano, M. W., Horlick, R. A., Springer, B. A., Van Dyk, D. E., Tobery, T., Wetmore, T. R., Lear, J. D., Nahapetian, A. T., Bradley, J. D., & Sisk, W. P. (1994) *Biochemistry 33*, 10229−10248.

Rapraeger, A. C., Krufka, A., & Olwin, B. B. (1991) *Science 252*, 1705−1708.

Shing, Y., Folkman, J., Sullivan, R., Butterfield, C., Murray, J., & Klagsbrun, M. (1984) *Science 223*, 1296−1299.

Williams, A. F., & Barclay, A. N. (1988) *Annu. Rev. Immunol. 6*, 381−405.

Xu, J., Nakahara, M., Crabb, J. W., Shi, E., Matuo, Y., Fraser, M., Kan, M., Hou, J., & McKeehan, W. L. (1992) *J. Biol. Chem. 267*, 17792−17803.

Yarden, Y., & Ullrich, A. (1988) *Annu. Rev. Biochem. 57*, 443−477.

Yayon, A., Klagsbrun, M., Esko, J. D., Leder, P., & Ornitz, D. M. (1991) *Cell 64*, 841−848.

Yayon, A., Zimmer, Y., Guo-Hong, S., Avivi, A., Yarden, Y., & Givol, D. (1992) *EMBO J. 11*, 1885−1890.

Yayon, A., Gray, T. E., Zimmer, Y., Eisenstein, M., & Givol, D. (1995) *J. Recept. Signal Transduction Res. 15*, 185−197.

Zimmer, Y., Givol, D., & Yayon, A. (1993) *J. Biol. Chem. 268*, 7899−7903.

BI951000S